

# An experimental study of non-destructive testing on glass fibre reinforced polymer composites after high velocity impact event

N Razali, M T H Sultan\* and F Cardona

Aerospace Manufacturing Research Centre (AMRC), Faculty of Engineering,  
Universiti Putra Malaysia, Malaysia.

\*thariq@upm.edu.my

**Abstract.** A non-destructive testing method on Glass Fibre Reinforced Polymer (GFRP) after high velocity impact event using single stage gas gun (SSGG) is presented. Specimens of C-type and E-type fibreglass reinforcement, which were fabricated with 6mm, 8mm, 10mm and 12mm thicknesses and size 100 mm x 100 mm, were subjected to a high velocity impact with three types of bullets: conical, hemispherical and blunt at various gas gun pressure levels from 6 bar to 60 bar. Visual observation techniques using a lab microscope were used to determine the infringed damage by looking at the crack zone. Dye penetrants were used to inspect the area of damage, and to evaluate internal and external damages on the specimens after impact. The results from visual analysis of the impacted test laminates were discussed and presented. It was found that the impact damage started with induced delamination, fibre cracking and then failure, simultaneously with matrix cracking and breakage, and finally followed by the fibres pulled out. C-type experienced more damaged areas compared to E-type of GFRP.

## 1. Introduction

When composites were introduced into aircraft components and aerospace industries, unexpected impacts occurred. These might be due to damages during flight operations such as runway debris on composite airframes, bird strike during flight operation and dropping of hand tools during maintenance work. For this research, the impact velocity is set to be less than 31 m/s, which indicates low velocity testing. For high velocity testing, the impact velocity is in the range of 31 m/s to 240 m/s. In this study, high velocity impact test has been chosen to be conducted on Glass Fibre Reinforced Polymer (GFRP) since this material has been used widely in many applications. The study of a high velocity impact comparison between two types of GFRP: durability (Type C) and electrical conductivity (Type E) has never been done before. This study is necessary to analyse the impact behaviour of GFRP in the form of chemical. When these materials are subjected to the high velocity impacts, their structural integrity, stiffness and also toughness are significantly reduced and this may result in a catastrophic failure to the structure in extreme scenarios. Matrix cracking, fibre fracture, fibre pullout and delamination are examples of major undetected hidden damages in composite materials after an event of impact. There is a need to study the behaviour of the composite materials under impact loading as the impacts occur mainly during maintenance and work manufacturing.



Optical microscopy (OM) as well as scanning electron microscopy (SEM) are classical techniques for composite surface studies [1–3]. From the observation, the types of failure can be determined and analyzed. A variety of failure modes after high impact velocity tests may lead to perforation of the composite panels. Failure modes of the target will vary depending on the properties of the materials, impact velocity, projectile nose shape, target geometry, support conditions, relative mass of projectile and target, etc. The most common failure modes are illustrate as in Figure 1.

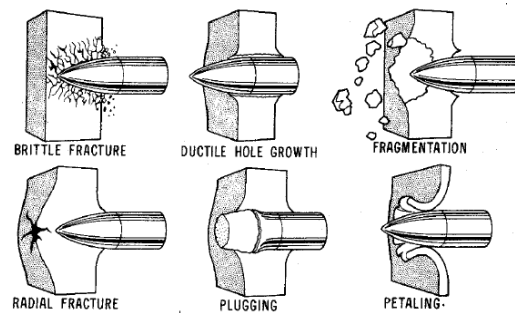


**Figure 1.** Common failure modes on the different type of materials [4]

The most significant failure modes in the present exploration are brittle fracture and petaling. A brittle fracture happens as a consequence of tensile stress acting typical to the crystallographic planes with low bonding when the bullets hits the surface material. Petaling failure happens when the rigidity is surpassed at the back side of the objective and a star-moulded break creates around the tip of the bullets. The parts shaped are then pushed back by the movement of bullets, framing petals as appeared in Figure 1. Matrix damage is the main sort of failure instigated by a transverse low-velocity impact. Typically, this appears as matrix breaking and de-bonding between the fibre and the matrix. Matrix breaks happen because of property confounding between the fibre and the matrix, and are typically situated in planes parallel to the fibre heading in the unidirectional layers. Delamination is a split that keeps running in resin-rich range between various fibre orientation and it is not between lamina in the same ply bunch. Delamination is an after-effect of bending mismatch coefficient between two nearby laminates such as diverse fibre orientations between the layers. The more the mismatch (0/90 degrees), the more delamination range will be [5]. The delamination will influence the materials' properties and it disrupts the stacking arrangement and the laminates thickness. Both bending splits and shear breaks could start delamination. Delamination initiated by shear breaks is precarious while the bending break prompts delamination to develop in a steady way in correspondence to the applied load. This damage mode generally happens much later in the break procedure than matrix splitting and delamination.

Fibre failure happens under the penetrators because of local high stresses and the space impacts of shear forces. It also occurs on the non-affected face because of high bending stresses. The fibre failure is a forerunner to the disastrous infiltration mode. Penetration is a plainly visible method of failure. It happens when the fibre failure achieves a basic degree, empowering the penetrators to totally infiltrate the material. It is anything but difficult to anticipate the introduction of matrix cracking fibre of the unidirectional layers while the break patterns of haphazardly situated layers are less simple to set up [6-8]. The aims of this research are to analyse the damage area and the effect of high velocity impact, and to observe the types of failure using non-destructive technique corresponding to the different types of bullets and impact energy level between the two types of GFRP using single stage gas gun (SSGG).

Various NDT techniques are used for damage detection in composite structures. Examples include acoustic emission technique (AE), ultrasonic testing, structural health monitoring, visual inspection technique, eddy current testing, holography and shearography imaging technique, vibration-based technique and lamb wave techniques. AE is a passive method that has been widely used as the NDT tool for damage detection in composite structures. AE analysis is a useful method for the investigation of local damage in materials. One of its advantages in comparison to the other NDE techniques is the possibility to observe the damage processes during the entire load history without any disturbance to

specimen. AE analysis is used successfully in a wide range of applications including for detecting and locating faults in the pressure vessels or leakage in storage tanks or pipe systems, monitoring welding applications, corrosion processes, partial discharges from components subjected to high voltage and the removal of protective coatings [9]. Ultrasonic testing uses high frequency sound energy to conduct examination and make measurements. The ultrasonic inspection can be applied for flaw detection or evaluation, dimensional measurements, material characterization and more [10].

Standard eddy current testing is essentially a near-surface technique, which is useful for detecting surface breaking or near-surface cracking and variations in material composition. It can also be used to measure the thickness of non-electrical conductive coatings on electrically conductive substrates. In general, standard eddy current methods are only used in plant inspection for nonferritic material where the eddy current penetration is deeper or for special applications such as inspection of heat exchanger tubing for cracking or corrosion thinning [11]. The vibration based model dependant methods with piezoelectric sensor and actuator incorporated into composite structures offer a promising option to fulfil such requirements and needs. These methods utilize finite element analysis techniques, together with experimental result, to detect damage. They locate and estimate the damage events by comparing dynamic responses between the damaged and undamaged structures. Meanwhile, holography is 'lens-less photography' in which the image is captured not as an image focused on film but instead as an interface pattern at the film. Typically, coherent light from a laser is reflected from an object and combined at the film light from a reference beam. This recorded interference pattern actually contains more information than a focused image and enables viewers to look at the appearance from several different angles, just as if looking at a real 3D object [12].

On the other hand, structural health monitoring is an upcoming technology in civil, mechanical and aerospace engineering. It is an approach used to monitor structure physical properties such as loading, stresses, strains, accelerations, cracks and etc. It is also a maintenance approach that can detect and identify global structural damage through automated continuous or periodical monitoring. Moreover, visual inspection is the most cost-effective method used for damage detection in aircraft structures. Visual inspection requires little equipment. Aside from good eyesight and sufficient light, all it takes is pocket rule, weld size gauge, magnifying glass, and possibly straight edge and square for checking straightness, alignment and perpendicularity [13]. Liquid penetrant inspection technique is a widely applied and low-cost inspection method used to locate the surface breaking defect in all non-porous material including metals, plastics, ceramics and composites. Penetrant may be applied to all non-ferrous materials but magnetic particle inspection is preferred for inspection of ferrous components due to its subsurface detection capability. Liquid penetrant inspection is used to detect casting and forging defects, cracks and leaks in new products, and fatigue cracks in service components. In this research, visual inspection techniques using a dye penetrant was used to observed the damage area and the mode of failure after high velocity impact.

## 2. Methodology

### 2.1. Specimens fabrication

GFRP of type E-glass and type C-glass are chosen for this research since they are easy to obtain and of low cost. Thermal properties of the fibre is one of the criteria that affect the material selection. Since this research is more concerned with high velocity impact, the material that can perform well in high application should be considered. Thus, the same materials are used for low velocity impact testing. Fibres made primarily from silica-based glass containing several metal oxides offer excellent thermal and impact resistance, high tensile strength, good chemical resistance and outstanding insulating properties. E-glass has a low thermal conductivity and is resistant to thermal shock. Fibreglass woven roving fabric also easier to fabricate compared to the chopped strand mat, giving it design flexibility. The manufacturing procedure for this GFRP consists of material preparation, a lay-up process, curing and CNC machine cutting. All specimens are oriented in the same  $0^{\circ}$  direction.

The GFRP woven cloth was first cut into large panels of 320 mm long and 320 mm wide. After the cutting process, the next step was to perform the lay-up preparation using a heat blanket machine. The laminates were fabricated for the impact tests with different thickness, i.e. 6, 8, 10 and 12 mm. The thickness of each plies of fibre had been measured before the fabrication. The estimation of number of layers had been made after a few sample had been fabricated. All of the fabricated specimens had the same fibre loading and matrix weight fraction. Epoxy resin was used as the matrix by the mixing of epoxy and hardener in 2:1 weight ratio. Both the epoxy and the hardener used were of type Zeepoxy HL002TA and Zeepoxy HL002 TB, respectively. The mixed epoxy-hardener had a low viscosity that allowed easy handling and provided good wetting of the glass reinforcements. The curing process for the high velocity impact test specimens involved the use of heat blanket machine Heatcon HCS9000B and vacuum bagging process. This method accelerated the curing process and also resulted in better strength of the composite material due to the pressure applied by the metallic plate that properly compacted the panel. The material was cured in the vacuum bagging for two hours at 150 °F (65.56°C) to ensure the resin flowed uniformly to the whole glass layers and that the resin fully cured inside the laminates. Each panel then was cut into nine specimens with the required dimensions of 100 × 100 mm as shown in Figure 2 using a CNC router machine.

### 2.2. Impact testing

The impact tests were carried out using a single stage gas gun as shown in Figure 3. The test machine consists of five main components: catch chamber, ballistic data acquisition system, pressure reservoir unit, firing mechanism unit and the launching unit. The catch chamber provides room for holding the specimen to be tested. The impact tests were performed by clamping the specimens between two steel frames at the catch chamber and striking them at the centre with a bullet.

The ballistic data acquisition system collected the data from the test such as the impact energy and the impact force. The pressure reservoir unit consists of a cylindrical gas tank, pressure regulator, a pressure vessel and a pressure control valves. This unit is used to control the pressure of the gas gun. The pressures were varied from 6 bar to a maximum of 60 bar. Varying the gas pressure in the firing chamber will proportionally vary the bullet velocity. Table 1 shows the details of gas pressures used according to the test panel's thickness. The applied gas pressure was varied due to the fact that thin panel samples were not able to withstand the high velocity impact (given by high gas pressure) and therefore, it was necessary to reduce the gas pressure to avoid complete damage of the panels by the total penetration of the bullets on impact. Initial impact pilot tests established the gas pressure to apply in accordance with the thickness of the test panels.

Figure 4 shows three different types of bullets used in this experiment: blunt, hemispherical and conical shape. Each bullet had different cross section area that would affect the impact test result. The bullets that had been used were made from stainless steel. All bullets had the same weight of 5 g. The dimensions of projectile used were 15 mm in length and 10 mm in diameter. The firing mechanism unit influenced the gun's performance by insuring that the bullet slid smoothly along the chamber and shot the target specimen.



**Figure 2.** GFRP specimens for high velocity impact testing



**Figure 3.** Single Stage Gas Gun (SSGG)



**Figure 4.** Type of bullet

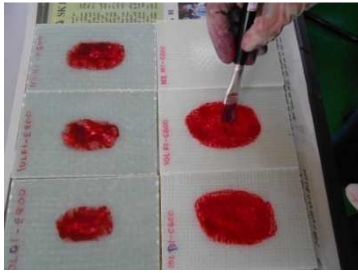


**Figure 5.** Dye penetrant applied on the surface of specimens using brush

**Table 1.** The pressure varied for each thickness of specimens

Thickness (mm)	Pressure (bar)		
	P <sub>1</sub>	P <sub>2</sub>	P <sub>3</sub>
6	6	12	18
8	10	20	30
10	15	30	45
12	20	40	60

The test was carried out by varying the pressure of the gas gun from 6 bar to 60 bar. Three projectiles of different geometries, which were blunt, hemispherical and conical, were impacted to the laminated specimen of 100 mm x 100 mm with 6 mm, 8 mm, 10 mm and 12 mm thickness. Each specimen was subjected to a single impact event.

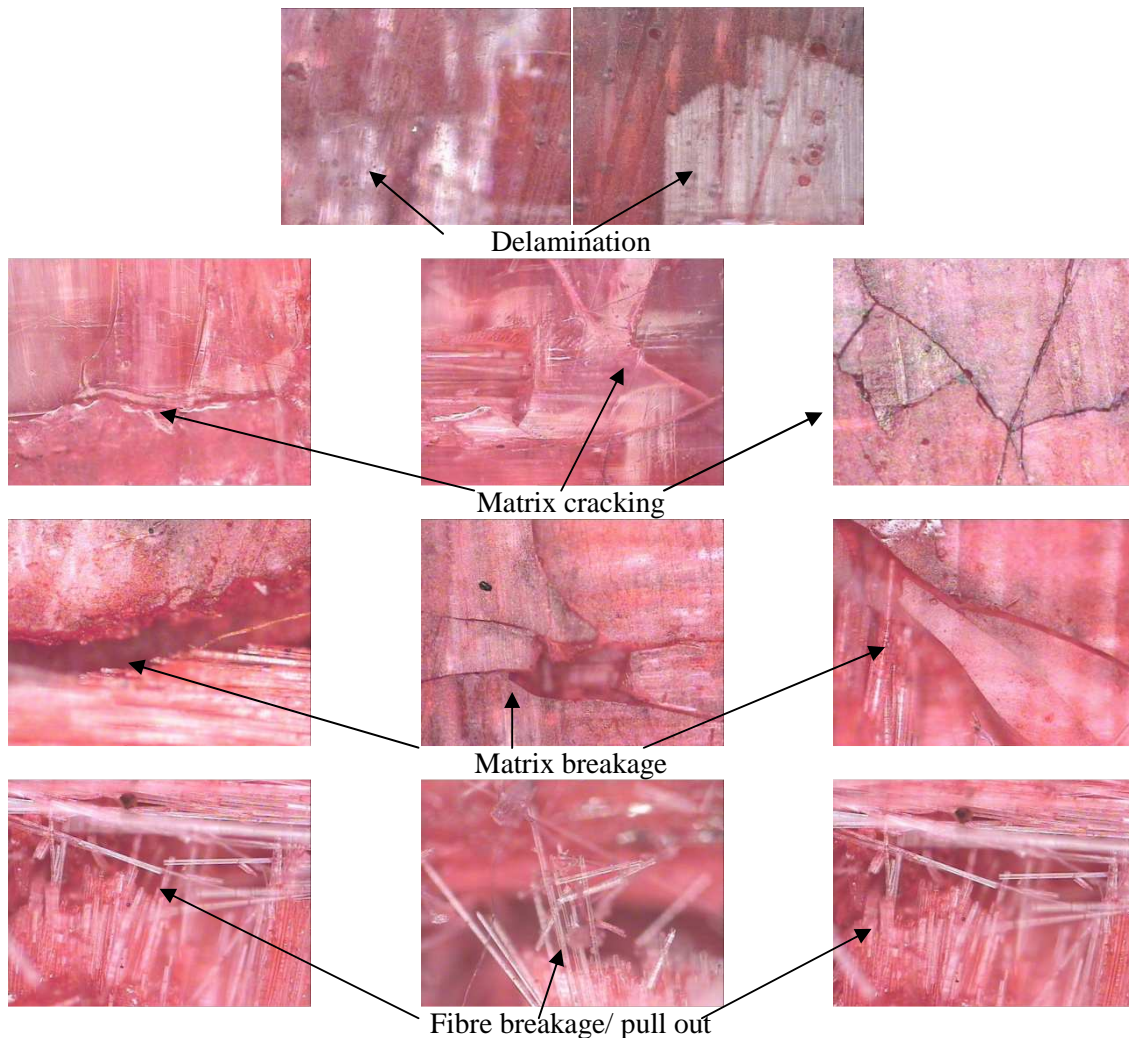
### 2.3. Non-destructive technique

There are many non-destructive techniques that can be used to examine impact damage of composite materials. One of the non-destructive techniques is by using a dye penetrant process. In this particular work, this technique was selected to examine the damage. In this experiment, Spotcheck SKL-SP2 dye penetrant was used. It is a red-colour contrast penetrant that is removable by solvent and with an outstanding penetrating characteristics. Thinner was used to clean the surface of the specimens from small debris and dirt. A synthetic cloth was used to wipe the surface. The dye penetrant was applied on the surface of the test specimens using a brush as shown in Figure 5, which was then left to dissipate through the damage area for 20 minutes. After 20 minutes, the specimens once again were wiped with the synthetic cloth and thinner to clean the surface. The damage area could be seen as the red colour of the dye contrasting with the colour of the specimens. As the damage areas were much clearer after the dye penetrant process, they will be easily examined using optical microscope. The optical microscope used in this examination was Olympus BX51 microscope, which can observed failure modes of the specimens over the impact zone. The advantages of using this optical microscope are its superb optical performance, optimised contrast and resolution, and outstanding fluorescent capability. The damage area was then calculated manually by grid paper.

### 3. Results and discussion

After the high velocity impact test was completed, the same non-destructive procedure techniques were performed on the tested specimens, which were the dye penetrant process and optical microscopic examination. Figure 6 shows the failure mode of the specimens after impact for both types of GFRP. Meanwhile, Figure 7 to Figure 19 show the surface of the GFRP laminates after impact by different types of bullets and with different applied gas pressure. The actual penetration of the bullets into the GFRP laminates was 70~80% maximum of the panel thickness, without going through the whole panels. After high velocity impact, all specimens underwent fibre breakage and fibre pullout as shown in Figure 6. Due to the high velocity impact event, the bullet penetrated through the surface of the specimens and broke the fibres, inducing a delamination, matrix cracking and matrix breakage on the side of the test specimens. The figures highlight that the bullets also created a hole on the impacted surface of the test specimens. The diameter of the damage area was increased as the applied gas gun pressure was increased. The impact damage started with induced delamination, fibre cracking and failure, simultaneously with matrix cracking and breakage, and finally followed by the fibres pulled out (see Figure 6). From the observation, Type E-glass/epoxy 600 g/m<sup>2</sup> laminates experienced the same failure as the type C-glass/epoxy 600 g/m<sup>2</sup> panels. The only main difference was that type C-panels suffered much larger and wider crack damage, and also much deeper bullet penetration than type E-panels. This shows that E-glass is tougher and stronger in comparison to C-glass. The visual

observation of the induced damage was much clearer after the dye-penetrant process. The recorded images of the impact areas showed similar damage conditions (impact area and penetration hole) for panels hit by the same type of bullets and with the same gas pressure, indicating a high grade of reproducibility and consistency on the high velocity impact tests. The micrographs also revealed that the increase in the gas gun pressure enhanced the damage sustained by the fibreglass and the whole composite structure. The results demonstrated that for the same applied gas pressure, the conical shape bullets penetrated deeper through the surface specimens than both hemispherical and blunt shaped bullets due to its smaller surface area.



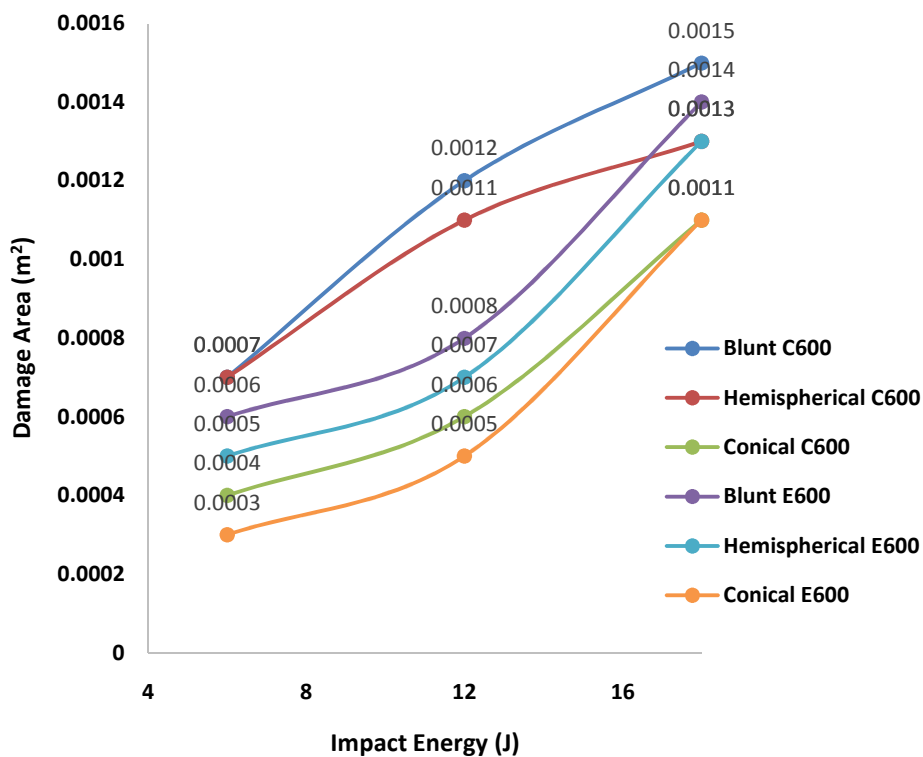
**Figure 6.** Failure modes of the test specimens (magnification power is 5 times)

Table 2 until Table 5 shows the data of damage area for all specimens impacted by the three types of bullets with different levels of impact energy. It also shows the failure mode experienced by the impacted specimens: fibre crack and fibre pull-out. The impacted specimens experienced delamination and matrix cracking as shown in Figure 6 before it turned to fibre breakage and fibre pull-out. Multiple matrix breakage extended at the back of the impacted area, and the fibre broke just beneath the impact point due to the high impact velocity. Extensive fibre cracks, which appeared as catastrophic failure, were generated beneath the impact point. Outside the ply failure zone, delamination occurred and extended from the tips of the matrix cracks. Most of the specimens suffered a fibre crack at the low impact energy while the higher impact energy caused the specimens to undergo fibre pull-out failure.

Figure 7 until Figure 10 illustrate the differences of impact area between type C and type E specimens. The graph also shows the differences of damage area using a different type of bullets. As can be seen in the figures, C600 had larger impact area compared to E600. From this results, it was concluded that the C-type suffered more damage than E-type. Blunt type of impactor had larger impact area, followed by hemispherical and conical. This is because of blunt type has larger cross section area compared to the other two. Conical type of bullet penetrated much deeper than the other bullets, hence its surface area had smaller damage.

**Table 2.** Damage area and mode of failure for 6 mm specimens

GFRP	Impact energy / failure	Type of bullets		
		Blunt	Hemispherical	Conical
C600	6	0.0007	0.0007	0.0004
		Fibre crack	Fibre crack	Fibre crack
	12	0.0012	0.0011	0.0006
		Fibre crack	Fibre crack	Fibre crack
	18	0.0015	0.0013	0.0011
		Fibre crack	Fibre crack	Fibre pull-out
E600	6	0.0006	0.0005	0.0003
		Fibre crack	Fibre crack	Fibre crack
	12	0.0008	0.0007	0.0005
		Fibre crack	Fibre crack	Fibre crack
	18	0.0014	0.0013	0.0011
		Fibre crack	Fibre crack	Fibre crack



**Figure 7.** Graph of damage area against impact energy for 6 mm specimens

**Table 3.** Damage area and mode of failure for 8 mm specimens

GFRP	Impact energy / failure	Type of bullets		
		Blunt	Hemispherical	Conical
C600	10	0.0012	0.0008	0.0007
		Fibre crack	Fibre crack	Fibre crack
	20	0.0014	0.0013	0.0013
		Fibre crack	Fibre crack	Fibre pull-out
	30	0.0016	0.0015	0.0013
		Fibre crack	Fibre pull-out	Fibre pull-out
E600	10	0.0010	0.0008	0.0007
		Fibre crack	Fibre crack	Fibre crack
	20	0.0012	0.0011	0.0011
		Fibre crack	Fibre crack	Fibre crack
	30	0.0014	0.0012	0.0011
		Fibre crack	Fibre crack	Fibre pull-out

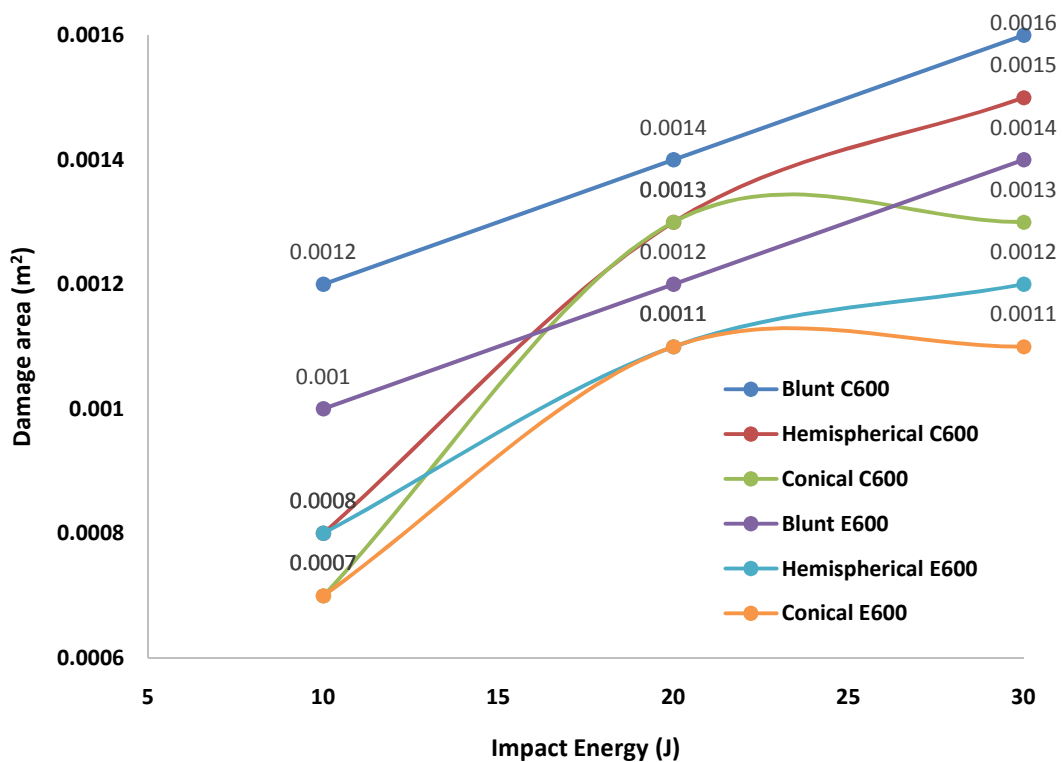


**Figure 8.** Graph of damage area against impact energy for 8 mm specimens

**Table 4.** Damage area and mode of failure for 10 mm specimens

GFRP	Impact energy / failure	Type of bullets		
		Blunt	Hemispherical	Conical
C600	15	0.0008	0.0007	0.0006
		Fibre crack	Fibre crack	Fibre pull-out
	30	0.0009	0.0008	0.0007
		Fibre crack	Fibre pull-out	Fibre pull-out
	45	0.0011	0.0010	0.0008
		Fibre crack	Fibre pull-out	Fibre pull-out
E600	15	0.0006	0.0005	0.0004
		Fibre crack	Fibre crack	Fibre pull-out
	30	0.0007	0.0007	0.0006
		Fibre crack	Fibre pull-out	Fibre pull-out
	45	0.0009	0.0007	0.0007
		Fibre crack	Fibre pull-out	Fibre pull-out

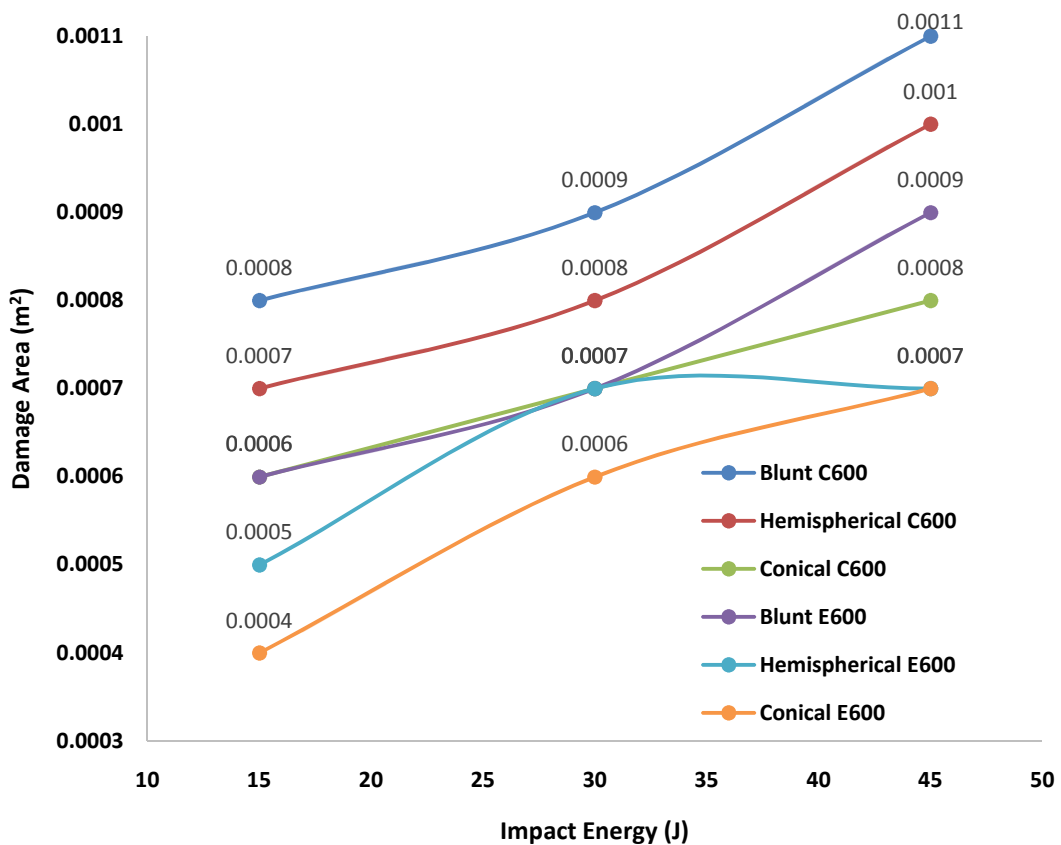


**Figure 9.** Graph of damage area against impact energy for 10 mm specimens

**Table 5.** Damage area and mode of failure for 12 mm specimens

GFRP	Impact energy / failure	Type of bullets		
		Blunt	Hemispherical	Conical
C600	20	0.0006	0.0006	0.0006
		Fibre pull-out	Fibre pull-out	Fibre pull-out
	40	0.0008	0.0007	0.0007
		Fibre pull-out	Fibre pull-out	Fibre pull-out
	60	0.0009	0.0008	0.0008
		Fibre pull-out	Fibre pull-out	Fibre pull-out
E600	20	0.0005	0.0004	0.0004
		Fibre pull-out	Fibre pull-out	Fibre pull-out
	40	0.0007	0.0005	0.0005
		Fibre pull-out	Fibre pull-out	Fibre pull-out
	60	0.0008	0.0007	0.0007
		Fibre pull-out	Fibre pull-out	Fibre pull-out

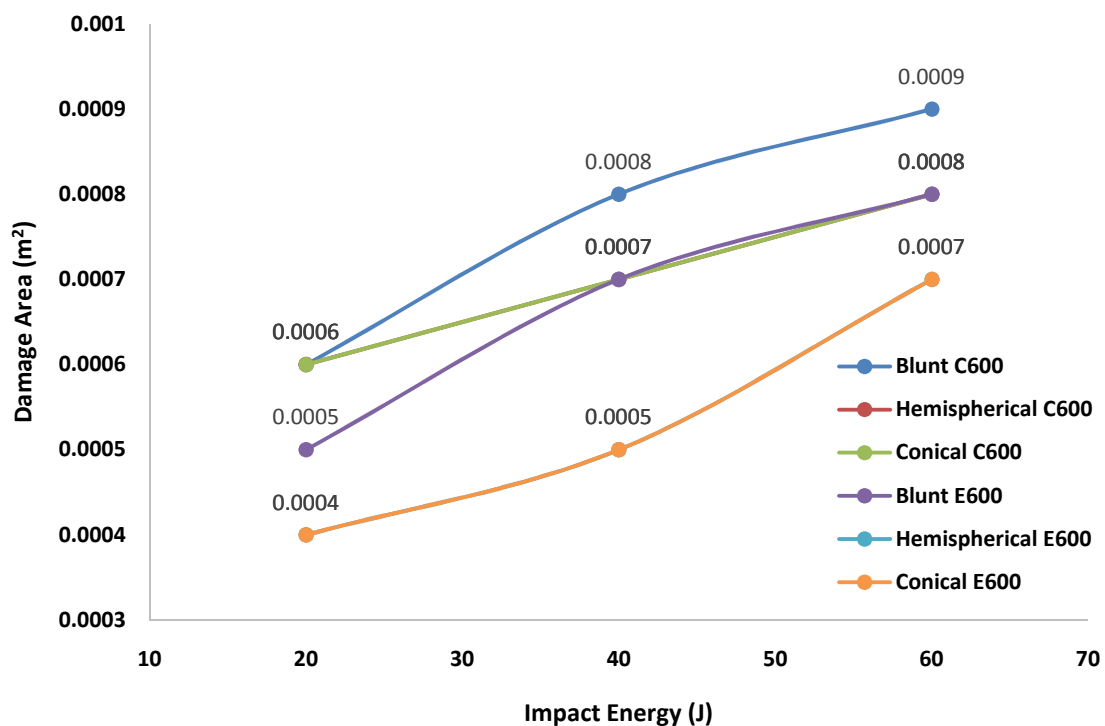


**Figure 10.** Graph of damage area against impact energy for 12 mm specimens

**4. Conclusion**

A non-destructive technique was used to evaluate impact damage and type of failure experienced by the C-glass and E-glass types of reinforced composite panels. The identified damage mechanism of the composite laminates after the high velocity impact tests involved delamination, matrix cracking and breakage with simultaneous fibre cracking and fibre breakage, and finally followed by the fibre pull-out. The increase in the applied gas gun pressure resulted in an increasing impact damage area of the panel’s surface. A general trend was observed. As the gas gun pressure was increased, initial velocity of the projectile also increased, the projectile kinetic energy increased, the maximum force exerted to specimens increased and the energy absorbed by the specimens also increased. Most of the impacted

specimens showed that the E-types experienced smaller damage area compared to C-types of GFRP. In this analysis, the character of impact damage can be divided into two parts: intra-laminar damage and inter-laminar damage. The intra-laminar damage corresponds to matrix cracking, fibre or matrix de-bonding and fibres breakages whereas the inter-laminar damage corresponds to delamination effect. Furthermore, another non-destructive technique such as ultrasonic C-scans and X-rays can be used to determine the failure in the damaged area. To investigate further the damage in the composite, the specimens can undergo destructive techniques to see the extent of the damage. Another material can be tested to see the damage behaviour. The same procedure discussed in this research work can be used for different types of material like carbon fibre, Kevlar, natural fibres etc. A better understanding about fibreglass with a different type of fibreglass and a different orientation should be performed in the future to examine the differences between impact energy and force with the existing specimens discussed in this research. It can be concluded that E-glass/Epoxy 600 g/m<sup>2</sup> is stronger and tougher than the C-glass/Epoxy 600 g/m<sup>2</sup> since it has greater mechanical properties. Therefore, type E-glass is recommended to be used in structural applications as compared with Type C-glass.

### Acknowledgement

This work is supported by UPM under GP-IPB grant, 9415402. The authors would like to express their gratitude and sincere appreciation to the Aerospace Manufacturing Research Centre (AMRC) and the Department of Aerospace Engineering, Universiti Putra Malaysia (UPM).

### References

- [1] David C, Sublet P, Auriol A and Rappeneau J 1964 *Carbon* **2** 139–48
- [2] Thornton P R 1967 *Scanning electron microscopy* (London: Chapman and Hall)
- [3] Pfrang A, Reznik B, Gerthsen D and Schimmel T 2003 *Carbon* **41** 179–98
- [4] Zukas J A, Nicholas T and Swift H F 1992 *Impact dynamics* (Malabar: Krieger Publishing)
- [5] Drzal L T, Herra-Franko P J and Hoe H 2000 *Comprehensive Composite Materials* (Amsterdam: Elsevier)
- [6] Sultan M T H and Rafie A S M 2010 *International Journal of Mechanical and Material Engineering* **5** 260-7
- [7] Sultan M T H 2011 *Impact Damage Characterisation in Composite Laminates* PhD Thesis University of Sheffield
- [8] Sultan M T H, Worden K, Staszewski W J and Hodzic A 2012 *Composites Science and Technology* **72** 1108-20
- [9] Duke J C and Henneke E G 1980 *The Fifth International Acoustic Emission Symposium*
- [10] Rose J L 1999 *Ultrasonic Waves in Solid Media* (Cambridge: Cambridge University Press)
- [11] The Welding Institute Website [Accessed on March 2016]
- [12] Ambu R, Aymerich F, Ginesu F and Priolo P 2006 *Composite Science and Technology* **66** 199-205
- [13] Pang J W C and Bond I P 2005 *Composite: Part A: Applied Science and Manufacturing* **36** 183-8